

Photon-jet correlations in pp and $p\bar{p}$ collisions

T. Pietrycki

*Institute of Nuclear Physics
PL-31-342 Cracow, Poland*

A. Szczurek

*Institute of Nuclear Physics
PL-31-342 Cracow, Poland
and*

*University of Rzeszów
PL-35-959 Rzeszów, Poland*

(Dated: November 17, 2018)

We compare results of the k_t -factorization approach and the next-to-leading order collinear-factorization approach for photon-jet correlations in pp and $p\bar{p}$ collisions at RHIC and Tevatron energies. We discuss correlations in the azimuthal angle as well as in the two-dimensional space of transverse momentum of photon and jet. Different unintegrated parton distributions (UPDF) are included in the k_t -factorization approach. The results depend on UPDFs used. The standard collinear approach gives cross section comparable to the k_t -factorization approach. For correlations of the photon and any jet the NLO contributions dominate at relatively small azimuthal angles as well as for asymmetric transverse momenta. For correlations of the photon with the leading jet (the one having the biggest transverse momentum) the NLO approach gives zero contribution at $\phi_- < \pi/2$ which opens a possibility to study higher-order terms and/or UPDFs in this region.

PACS numbers: 12.38.Bx, 13.60.Hb, 13.85.Qk

I. INTRODUCTION

The jet-jet correlations are interesting probe of QCD dynamics [1]. Recent studies of hadron-hadron correlations at RHIC [2] open a new possibility to study the dynamics of jet and particle production. The hadron-hadron correlations involve both jet-jet correlations as well as complicated jet structure. Recently a preliminary data on photon-hadron azimuthal correlation in nuclear collisions were also presented [3]. In principle, such correlations should be easier for theoretical description as here only one jet enters, at least in leading order pQCD. On the experimental side, such measurements are more difficult due to much reduced statistics as compared to the dijet studies.

Up to now no theoretical calculation for photon-jet were presented in the literature, even for elementary collisions. In leading-order collinear-factorization approach the photon and the associated jet are produced back-to-back. If transverse momenta of partons entering the hard process are included, the transverse momenta of the photon and the jet are no longer balanced and finite (non-zero) correlations in a broad range of relative azimuthal angle and/or in lengths of transverse momenta of the photon and the jet are obtained. The finite cor-

relations can be also obtained in higher-order collinear-factorization approach [4]. According to our knowledge no detailed studies for present accelerators were presented in the literature.

In contrast to the coincidence studies the inclusive distributions of photons were studied carefully in pQCD up to the next-to-leading order [5]. Similar studies were performed recently also in the k_t -factorization approach [6, 7]. A rather good description of direct-photon inclusive cross sections can be obtained in both approaches. The k_t -factorization approach offers a relatively easy method to calculate the photon-jet correlations [6].

The k_t -factorization approach was used recently to several high-energy reactions, including heavy quark pair photo- [8, 9] and hadroproduction [10, 11], charmonium production [12, 13], inclusive Z_0 [14] and Higgs [15, 16] production.

In the present paper we shall compare results obtained in the leading-order k_t -factorization approach and the next-to-leading order collinear-factorization approach. We shall discuss which approach is more adequate for the different regions of phase space. We shall present corresponding results for proton-proton scattering at RHIC and proton-antiproton scattering at Tevatron.

II. FORMALISM

A. $2 \rightarrow 2$ contributions with unintegrated parton distributions

It is known that at midrapidities and at relatively small transverse momenta the photon-jet production is dominated by (sub)processes initiated by gluons. In Fig.1 we show basic diagrams which appear in the k_t -factorization approach to photon-jet correlations.

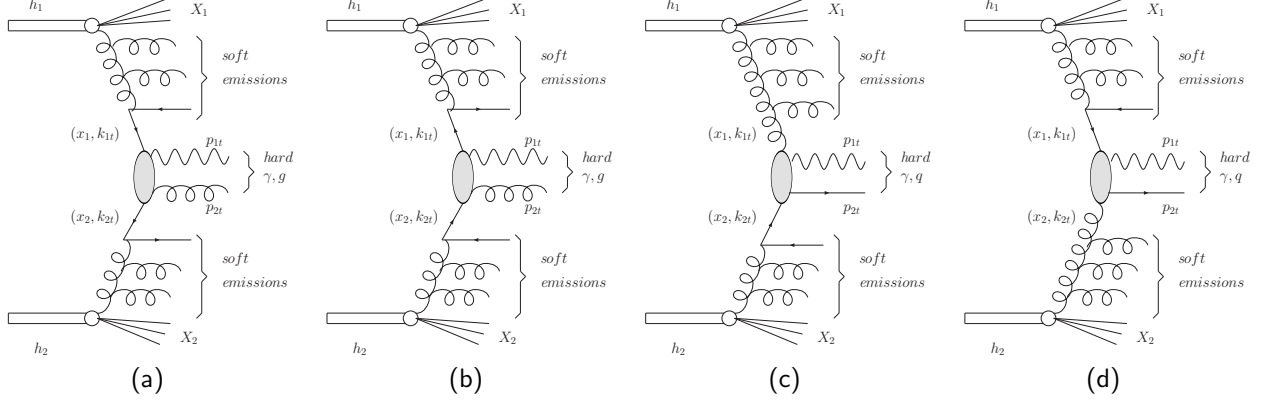


FIG. 1: Basic diagrams of k_t -factorization approach to photon-jet correlations.

In the k_t -factorization approach the cross section for a simultaneous production of a photon and an associated jet in the collisions of two hadrons (pp or $pp\bar{}$) can be written as

$$\frac{d\sigma_{h_1 h_2 \rightarrow \gamma k}}{d^2 p_{1,t} d^2 p_{2,t}} = \int dy_1 dy_2 \frac{d^2 k_{1,t}}{\pi} \frac{d^2 k_{2,t}}{\pi} \frac{1}{16\pi^2 (x_1 x_2 s)^2} |\overline{\mathcal{M}}_{ij \rightarrow \gamma k}|^2 \cdot \delta^2(\vec{k}_{1,t} + \vec{k}_{2,t} - \vec{p}_{1,t} - \vec{p}_{2,t}) \mathcal{F}_i(x_1, k_{1,t}^2, \mu_1^2) \mathcal{F}_j(x_2, k_{2,t}^2, \mu_2^2), \quad (1)$$

where $\mathcal{F}_i(x_1, k_{1,t}^2, \mu_1^2)$ and $\mathcal{F}_j(x_2, k_{2,t}^2, \mu_2^2)$ are so-called unintegrated parton distributions. The longitudinal momentum fractions are evaluated as

$$\begin{aligned} x_1 &= (m_{1t} e^{+y_1} + m_{2t} e^{+y_2}) / \sqrt{s}, \\ x_2 &= (m_{1t} e^{-y_1} + m_{2t} e^{-y_2}) / \sqrt{s}. \end{aligned} \quad (2)$$

We shall return to the choice of the factorization scale in the next section. Its role is completely different in different approaches i.e. different choices of UPDFs. A special attention will be devoted to the Kwieciński UPDF and the role of the scale parameter.

If one makes the following replacement

$$\begin{aligned} \mathcal{F}_i(x_1, k_{1,t}^2) &\rightarrow x_1 p_i(x_1) \delta(k_{1,t}^2), \\ \mathcal{F}_j(x_2, k_{2,t}^2) &\rightarrow x_2 p_j(x_2) \delta(k_{2,t}^2) \end{aligned} \quad (3)$$

then one recovers the standard leading-order collinear formula.

The final partonic state is $\gamma k = \gamma g, \gamma q$. The matrix elements for corresponding processes are discussed in Appendix A.

The inclusive invariant cross section for direct photon production can be written as

$$\frac{d\sigma_{h_1 h_2 \rightarrow \gamma}}{dy_1 d^2 p_{1,t}} = \int dy_2 \frac{d^2 k_{1,t}}{\pi} \frac{d^2 k_{2,t}}{\pi} (\dots) \Big|_{\vec{p}_{2,t} = \vec{k}_{1,t} + \vec{k}_{2,t} - \vec{p}_{1,t}} \quad (4)$$

and analogously the cross section for the associated parton (jet) can be written as

$$\frac{d\sigma_{h_1 h_2 \rightarrow k}}{dy_1 d^2 p_{1,t}} = \int dy_2 \frac{d^2 k_{1,t}}{\pi} \frac{d^2 k_{2,t}}{\pi} (\dots) \Big|_{\vec{p}_{1,t} = \vec{k}_{1,t} + \vec{k}_{2,t} - \vec{p}_{2,t}}. \quad (5)$$

Let us return to the coincidence cross section. The integration with the Dirac delta function in Eq.(1)

$$\int dy_1 dy_2 \frac{d^2 k_{1,t}}{\pi} \frac{d^2 k_{2,t}}{\pi} (\dots) \delta^2(\dots) \quad (6)$$

can be performed by introducing the following new auxiliary variables:

$$\begin{aligned} \vec{Q}_t &= \vec{k}_{1,t} + \vec{k}_{2,t} , \\ \vec{q}_t &= \vec{k}_{1,t} - \vec{k}_{2,t} . \end{aligned} \quad (7)$$

Then our initial cross section can be written as:

$$\frac{d\sigma_{h_1 h_2 \rightarrow \gamma, \text{parton}}}{d^2 p_{1,t} d^2 p_{2,t}} = \frac{1}{4} \int dy_1 dy_2 \frac{1}{2} dq_t^2 d\phi_{q_t} (\dots) |_{\vec{Q}_t = \vec{P}_t} . \quad (8)$$

Above $\vec{P}_t = \vec{p}_{1,t} + \vec{p}_{2,t}$. The factor $\frac{1}{4}$ before integrand on the rhs comes from the Jacobian of the $(\vec{k}_{1,t}, \vec{k}_{2,t}) \rightarrow (\vec{Q}_t, \vec{q}_t)$ transformation (see [6]).

B. $2 \rightarrow 3$ contributions in NLO collinear-factorization approach

Up to now we have concentrated only on processes with two explicit hard partons (γk) in the k_t -factorization approach. It is of interest to compare the results of our approach with those of the standard collinear next-to-leading order approach. In this section we discuss processes with three explicit hard partons. In Fig.2 we show diagrams for $2 \rightarrow 3$ subprocesses included in our calculations. In the following we assume particle No.1 to be a photon. Then particle No.2 is g, q and \bar{q} , depending on the subprocess.

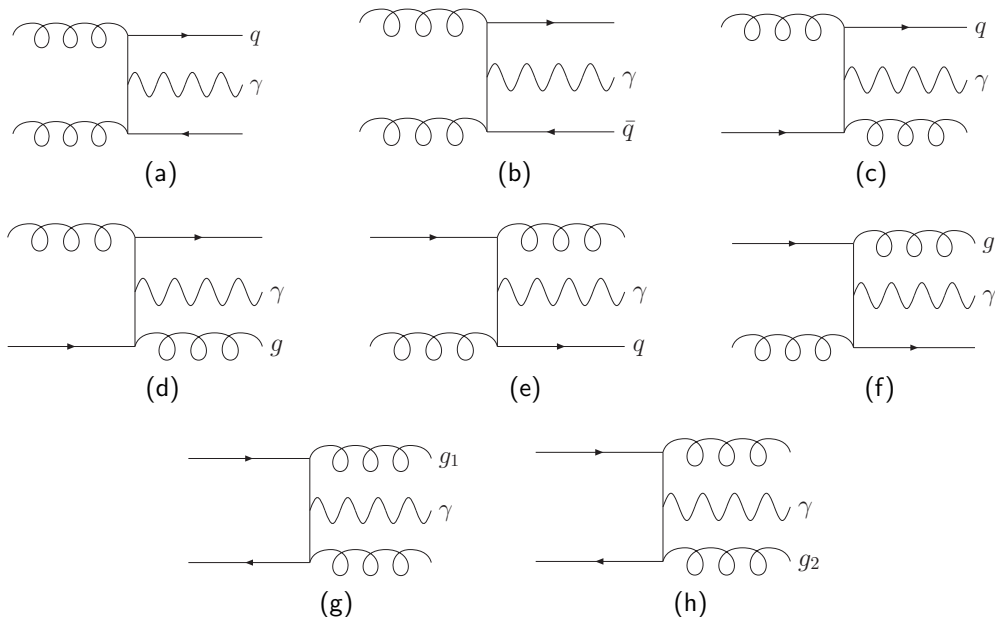


FIG. 2: Diagrams for NLO collinear-factorization approach for photon-jet-jet production.

The cross section for $h_1 h_2 \rightarrow \gamma klX$ processes can be calculated according to the standard parton model formula

$$d\sigma_{h_1 h_2 \rightarrow \gamma kl} = \sum_{ijk} \int dx_1 dx_2 p_i(x_1, \mu^2) p_j(x_2, \mu^2) d\hat{\sigma}_{ij \rightarrow \gamma kl} . \quad (9)$$

The elementary cross section can be written as

$$d\hat{\sigma}_{ij \rightarrow \gamma kl} = \frac{1}{2\hat{s}} |\overline{\mathcal{M}}_{ij \rightarrow \gamma kl}|^2 dR_3 , \quad (10)$$

where the three-body phase space element reads

$$dR_3 = (2\pi)^4 \delta^4(p_a + p_b - \sum_{i=1}^3 p_i) \prod_{i=1}^3 \frac{d^3 p_i}{2E_i (2\pi)^3}. \quad (11)$$

This element can be expressed in an equivalent way in terms of parton rapidities

$$dR_3 = (2\pi)^4 \delta^4(p_a + p_b - \sum_{i=1}^3 p_i) \prod_{i=1}^3 \frac{dy_i d^2 p_{i,t}}{(4\pi)(2\pi)^2}. \quad (12)$$

The last formula is useful for practical applications. Now the cross section for hadronic collisions can be written in terms of $2 \rightarrow 3$ matrix element as

$$d\sigma = \sum_{ijkl} dy_1 d^2 p_{1,t} dy_2 d^2 p_{2,t} dy_3 \frac{1}{(4\pi)^3 (2\pi)^2} \frac{1}{\hat{s}^2} x_1 p_i(x_1, \mu^2) x_2 p_j(x_2, \mu^2) \overline{|\mathcal{M}_{ij \rightarrow \gamma kl}|^2}, \quad (13)$$

where the longitudinal momentum fractions are evaluated as

$$\begin{aligned} x_1 &= \frac{1}{\sqrt{s}} \sum_{i=1}^3 p_{i,t} e^{+y_i}, \\ x_2 &= \frac{1}{\sqrt{s}} \sum_{i=1}^3 p_{i,t} e^{-y_i}. \end{aligned} \quad (14)$$

Repeating similar steps as for $2 \rightarrow 2$ processes we get finally

$$d\sigma = \sum_{ijkl} \frac{1}{64\pi^4 \hat{s}^2} x_1 p_i(x_1, \mu^2) x_2 p_j(x_2, \mu^2) \overline{|\mathcal{M}_{ij \rightarrow \gamma kl}|^2} p_{1,t} dp_{1,t} p_{2,t} dp_{2,t} d\phi_- dy_1 dy_2 dy_3, \quad (15)$$

where the relative azimuthal angle between the photon and the associated jet (ϕ_-) is restricted to the interval $(0, \pi)$. The last formula is very useful in calculating the cross section for particle 1 and particle 2 correlations.

III. RESULTS

In this section we shall present results for RHIC and Tevatron energies. We use UPDFs from the literature. There are only two complete sets of UPDF in the literature which include not only the gluon distributions but also the distributions of quarks and antiquarks:

- (a) Kwieciński [17],
- (b) Kimber-Martin-Ryskin [18].

For comparison we shall include also the unintegrated parton distributions obtained from the collinear ones by the Gaussian smearing procedure. Such a procedure is often used in the context of direct photons [19, 20]. Comparing results obtained with those Gaussian distributions and the results obtained with the Kwieciński distributions with nonperturbative Gaussian form factors will allow to quantify the effect of UPDF evolution as contained in the Kwieciński evolution equations. What is the hard scale for our process? In our case the best candidate for the scale is the photon and/or jet transverse momentum. Since we are interested in rather small transverse momenta the evolution length is not too large and the deviations from initial k_t -distributions (assumed here to be Gaussian) should not be too big.

At high energies one enters into a small- x region, i.e. the region of a specific dynamics of the QCD emissions. In this region only unintegrated distributions of gluons exist in the literature. In our case the dominant contributions come from QCD-Compton *gluon - quark* or *quark - gluon* initiated hard subprocesses. This means that we need unintegrated distributions of both gluons and quarks/antiquarks. In this case we take such UGDFs from the literature and supplement them by the Gaussian distributions of quarks/antiquarks.

Let us start from presenting our results on the $(p_{1,t}, p_{2,t})$ plane. In Fig.3 we show the maps for different UPDFs used in the k_t -factorization approach as well as for NLO collinear-factorization approach for $p_{1,t}, p_{2,t} \in (5, 20)$ GeV and at the Tevatron energy $W = 1960$ GeV. In the case of the Kwieciński distribution we have taken $b_0 = 1$ GeV⁻¹ for the exponential nonperturbative form factor and the scale parameter $\mu^2 = 100$ GeV². Rather similar distributions are obtained for different UPDFs. The distribution obtained in the NLO approach differs qualitatively from those

obtained in the k_t -factorization approach. First of all, one can see a sharp ridge along the diagonal $p_{1,t} = p_{2,t}$. This ridge corresponds to a soft singularity when the unobserved parton has very small transverse momentum $p_{3,t}$. As will be clear in a moment this corresponds to the azimuthal angle between the photon and the jet being $\phi_- = \pi$. Obviously this is a region which cannot be reliably calculated in collinear pQCD. There are different practical possibilities to exclude this region from the calculations. The most primitive way (possible only in theoretical calculations) is to impose a lower cut on transverse momentum of the unobserved parton $p_{3,t}$. Secondly, the standard collinear NLO approach generates much bigger cross section at configurations asymmetric in $p_{1,t}$ and $p_{2,t}$. We shall return to this observation in the course of this paper.

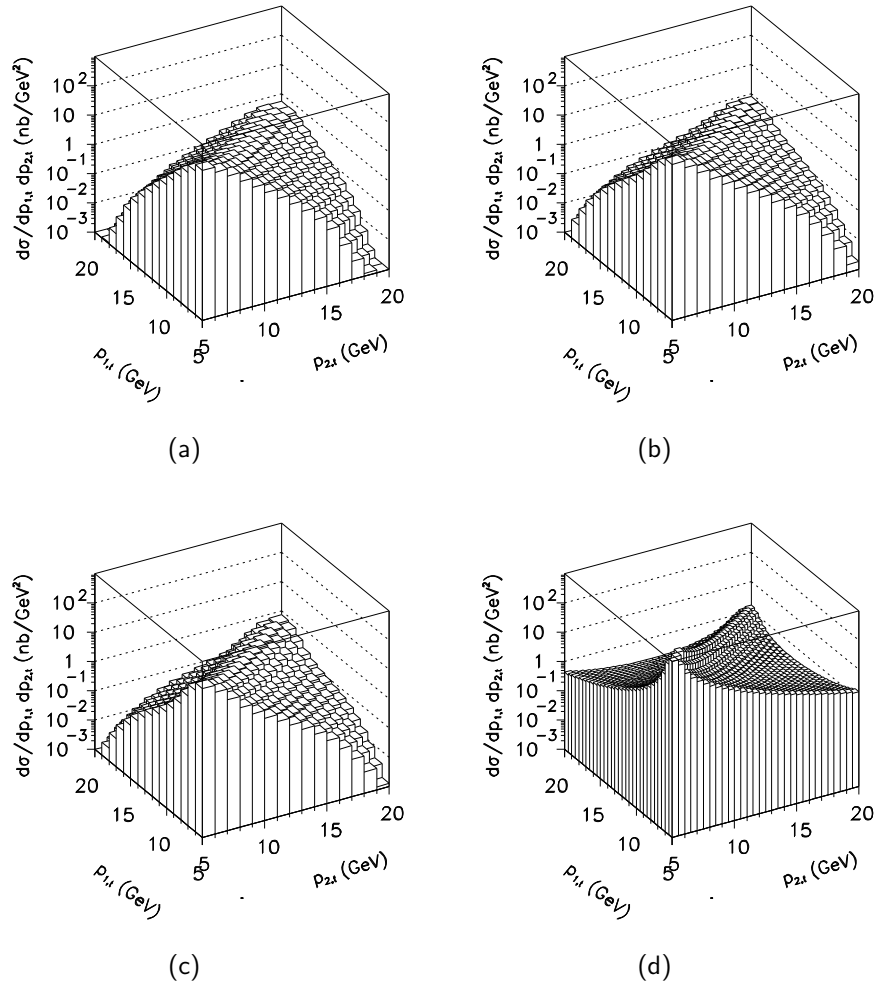


FIG. 3: Transverse momentum distributions $d\sigma/dp_{1,t}dp_{2,t}$ at $W = 1960$ GeV and for different UPDFs in the k_t -factorization approach for Kwieciński ($b_0 = 1\text{GeV}^{-1}$, $\mu^2 = 100\text{GeV}^2$) (a), BFKL (b), KL (c) and NLO $2 \rightarrow 3$ collinear-factorization approach including diagrams from Fig.2 (d). The integration over rapidities from the interval $-5 < y_1, y_2 < 5$ is performed.

As discussed in Ref.[6] the Kwieciński distributions are very useful to treat both the nonperturbative (intrinsic nonperturbative transverse momenta) and the perturbative (QCD broadening due to parton emission) effects on the same footing. In Fig.4 we show the effect of the scale evolution of the Kwieciński UPDFs on the azimuthal angle correlations between the photon and the associated jet. We show results for different initial conditions ($b_0 = 0.5, 1.0, 2.0 \text{ GeV}^{-1}$). At the initial scale (fixed here as in the original GRV [21] to be $\mu^2 = 0.25 \text{ GeV}^2$) there is a sizeable difference of the results for different b_0 . The difference becomes less and less pronounced when the scale increases. At $\mu^2 = 100 \text{ GeV}^2$ the differences practically disappear. This is due to the fact that the QCD-evolution broadening of the initial parton transverse momentum distribution is much bigger than the typical initial nonperturbative transverse momentum scale.

In Fig.5 we show corresponding azimuthal angular correlations. In this case integration is made over transverse

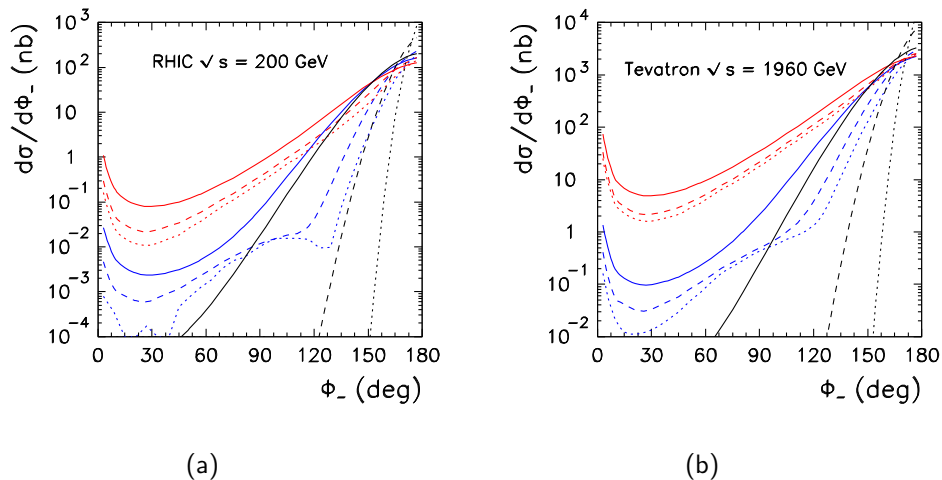


FIG. 4: (Color on line) Azimuthal angle correlation functions at (a) RHIC, (b) Tevatron energies for different scales and different values of b_0 of the Kwieciński distributions. The solid line is for $b_0 = 0.5 \text{ GeV}^{-1}$, the dashed line is for $b_0 = 1 \text{ GeV}^{-1}$ and the dotted line is for $b_0 = 2 \text{ GeV}^{-1}$. Three different values of the scale parameters are shown: $\mu^2 = 0.25, 10, 100 \text{ GeV}^2$ (the bigger the scale the bigger the decorrelation effect, different colors on line). In this calculation $p_{1,t}, p_{2,t} \in (5, 20) \text{ GeV}$ and $y_1, y_2 \in (-5, 5)$.

momenta $p_{1,t}, p_{2,t} \in (5, 20) \text{ GeV}$ and rapidities $y_1, y_2 \in (-5, 5)$.

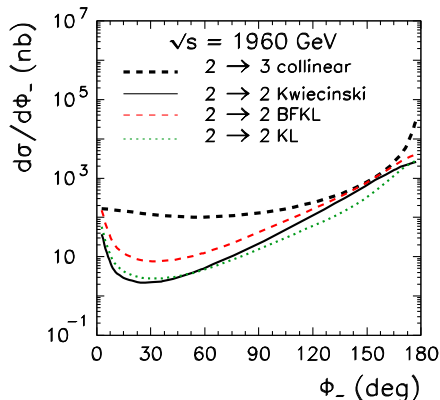


FIG. 5: Photon-jet angular azimuthal correlations $d\sigma/d\phi_-$ for proton-antiproton collision at $W = 1960 \text{ GeV}$ for different UPDFs in the k_t -factorization approach for the Kwieciński (solid), BFKL (dashed), KL (dotted) UPDFs/UGDFs and for the NLO collinear-factorization approach (thick dashed). Here $y_1, y_2 \in (-5, 5)$.

The singularity in NLO pQCD at $\phi_- = \pi$ is strongly correlated with the sharp ridge in Fig.3 d. This is demonstrated in Fig.6 where we present the results of azimuthal correlation function obtained for different cuts on $p_{3,t}$. The cut modifies only the region of relative azimuthal angles close to π . We wish to stress in this context that there are no singularities of the ridge type in the k_t -factorization approach.

The small transverse momenta of the unobserved jet contribute to the sharp ridge along the diagonal $p_{1,t} = p_{2,t}$. It is therefore difficult to distinguish these three-parton states from the states with two partons. The ridge can be eliminated in calculation by imposing a cut on the transverse momentum of the third (unobserved) parton. In experiments there is no possibility to impose such cuts and other methods must be used. We shall return to this point later in this paper.

In Fig.7 we show angular azimuthal correlations for different relations between transverse momenta of outgoing photon and partons: (a) with no constraints on $p_{3,t}$, (b) the case where $p_{2,t} > p_{3,t}$ condition (called leading jet

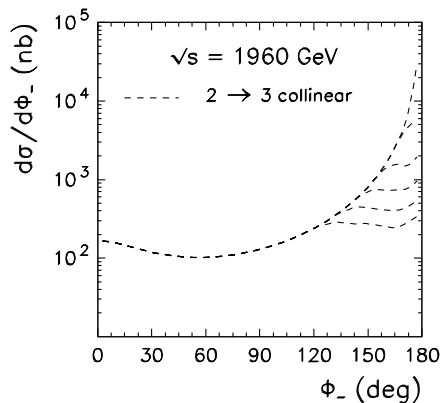


FIG. 6: Photon-jet angular azimuthal correlations $d\sigma/d\phi_-$ for proton-antiproton collision at $W = 1960$ GeV for the NLO collinear-factorization approach and different cuts on $p_{3,t}$. Here $y_1, y_2 \in (-5, 5)$.

condition in the following) is imposed, (c) $p_{2,t} > p_{3,t}$ and an additional condition $p_{1,t} > p_{3,t}$. The results depend significantly on the scenario as can be seen from the figure.

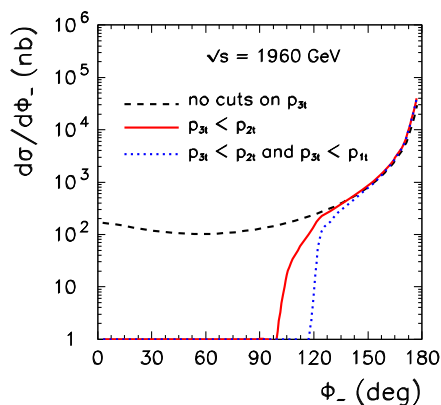


FIG. 7: Angular azimuthal correlations for different cuts on the transverse momentum of third (unobserved) parton in the NLO collinear-factorization approach without any extra constraints (dashed), $p_{3,t} < p_{2,t}$ (solid), $p_{3,t} < p_{2,t}$ and $p_{3,t} < p_{1,t}$ in addition (dotted). Here $y_1, y_2 \in (-5, 5)$.

In Fig.8 we show transverse momentum distribution $d\sigma/dp_{1,t}dp_{2,t}$ for the same extra conditions imposed before in Fig.7 for azimuthal angle correlations. Imposing the condition that the associated jet is the leading jet ($p_{2,t} > p_{3,t}$) causes that the large part of the phase space $p_{1,t} < 2p_{2,t}$ is not available in the next-to-leading approach. If one imposes in addition that $p_{1,t}(\text{photon}) > p_{3,t}(\text{unobserved jet})$ then also the $p_{2,t} < 2p_{1,t}$ region becomes excluded for the NLO approach. These NLO-excluded regions are therefore regions sensitive to higher-order corrections in pQCD.

In general, the correlations between the photon and the jet depend strongly on all kinematical variables - transverse momenta, azimuthal angles, etc. In order to expose this better, in Fig.9 we define windows in the $(p_{1,t}, p_{2,t})$ plane which will be used in the following to study the azimuthal correlations. At lower energies (as for RHIC) a region of rather low transverse momenta is more adequate (left figure). At larger energies (as for Tevatron) also region of somewhat larger transverse momenta can be of interest (right figure). The notation shown in the figure will be used for brevity in the rest of this paper for easy reference.

In Fig.10 we show angular azimuthal correlations $d\sigma/d\phi_-$ at RHIC energy $\sqrt{s} = 200$ GeV for the Kwieciński UPDFs in the k_t -factorization approach with on-shell and off-shell matrix elements and for the NLO collinear-factorization approach with extra leading jet condition $p_{3,t} < p_{2,t}$. Here transverse momentum of the photon and that of the

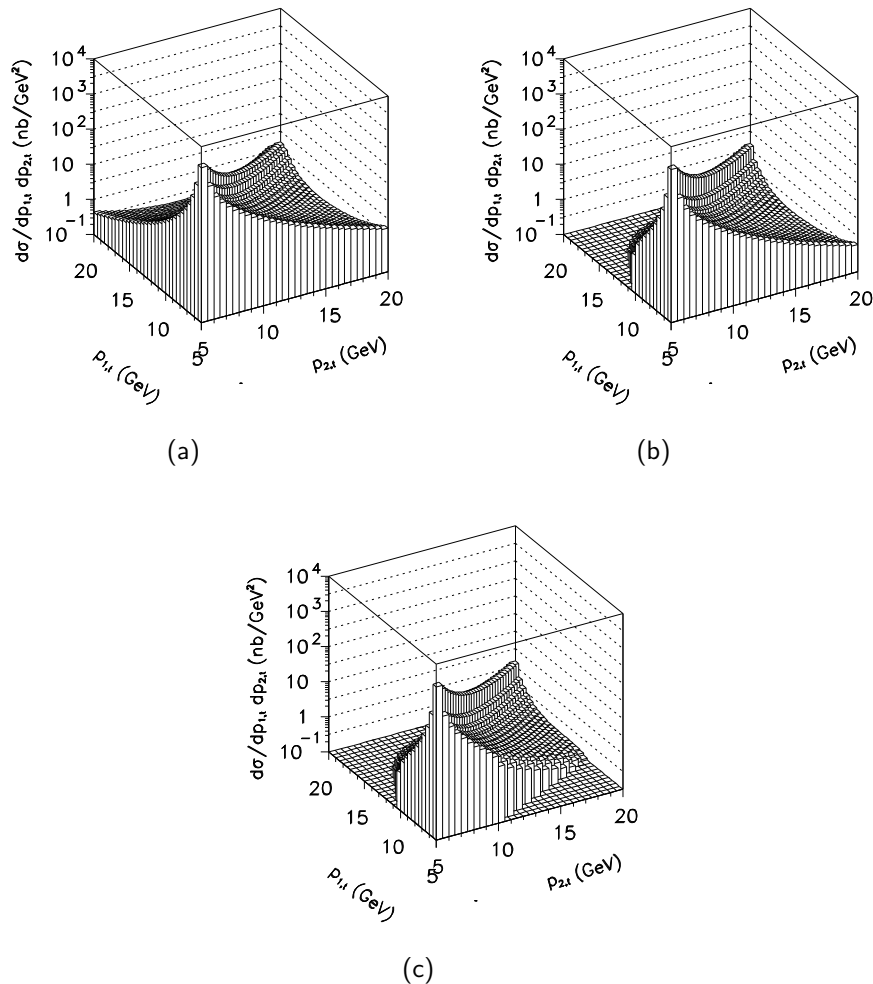


FIG. 8: Transverse momenta distribution $d\sigma/dp_{1,t}dp_{2,t}$ for different constraints on the transverse momentum of third (un-observed) parton in the NLO collinear-factorization approach with no constraints on $p_{3,t}$ (a), $p_{3,t} < p_{2,t}$ (b), $p_{3,t} < p_{2,t}$ and $p_{3,t} < p_{1,t}$ (c). All $2 \rightarrow 3$ processes shown in Fig.2 were included. Here $y_1, y_2 \in (-5, 5)$.

associated jet $p_{1,t}, p_{2,t}$ belong to the interval (5, 20) GeV. There is almost no difference between results obtained with off-shell and on-shell (see Appendix A) matrix elements.

In Fig.11 we show analogous angular distributions as in Fig.10 but for Tevatron energy $\sqrt{s} = 1960$ GeV. In Fig.12 we show angular correlations for a restricted range of rapidities $|y_1|, |y_2| < 0.9$ (corresponding to the present Tevatron apparatus) of the photon and the correlated jet. Limiting to midrapidities does not change the shape of azimuthal correlations significantly.

In Fig.13 we show similar distributions as in Fig.11 but for transverse-momentum windows spanned over broader range of transverse momenta $p_{1,t}, p_{2,t} \in (20, 80)$ GeV for the photon and the jet. We observe slightly faster decrease of the k_t -factorization cross sections for larger $p_{1,t}$ and $p_{2,t}$.

The standard collinear approach can be applied only in the region which is free of singularities. In order to eliminate the regions where the pQCD calculation is not reliable some cuts on the measured transverse momenta must be applied. The simplest method is to use cuts shown in Fig.14. Mathematically this means that $p_{1,t} > p_{cut}$, $p_{2,t} > p_{cut}$ and

$$|p_{1,t} - p_{2,t}| > \Delta_S. \quad (16)$$

We shall call the last cut a scalar cut for further easy reference. In Fig.15 we show azimuthal angle correlation function for different values of the scalar cut $\Delta_S = 0, 1, 2, 3$ GeV. Clearly the NLO singularity at $\phi_- = \pi$ can be removed by imposing the cut. However, the cut lowers also the k_t -factorization cross section.

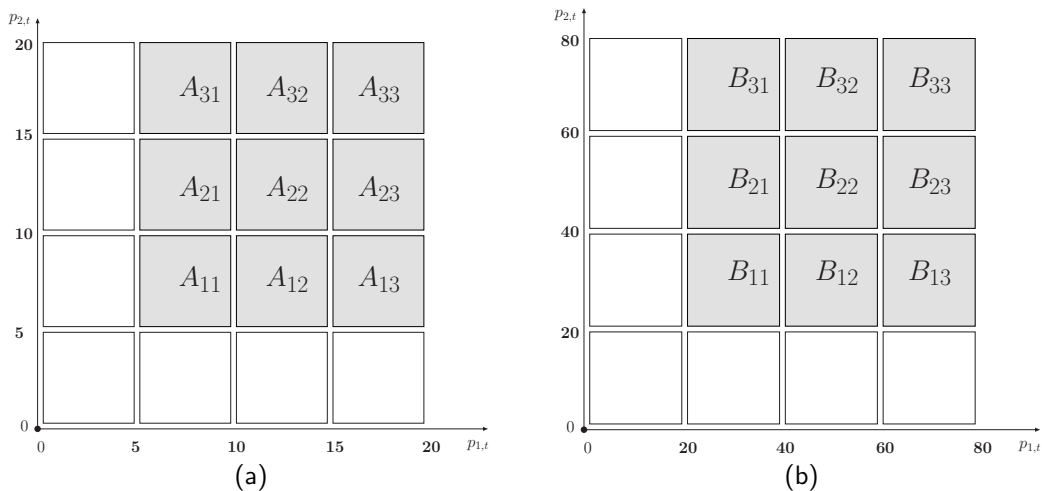


FIG. 9: The definition of the windows in $(p_{1,t}, p_{2,t})$ plane for RHC energy $\sqrt{s} = 200$ GeV (a) and for Tevatron energy $\sqrt{s} = 1960$ GeV (b).

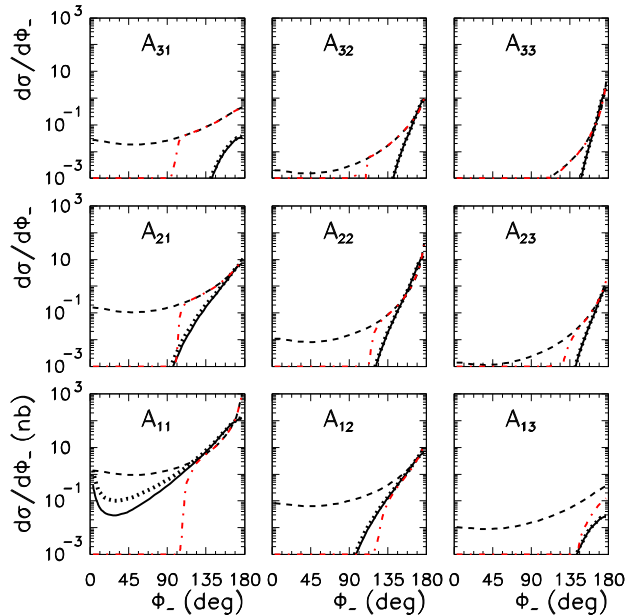


FIG. 10: Angular azimuthal correlations $d\sigma/d\phi_-$ at $\sqrt{s} = 200$ GeV for Kwieciński on-shell ME (solid), Kwieciński off-shell ME (thick dotted), NLO collinear with no cuts on $p_{3,t}$ (dashed) and NLO collinear with cut on $p_{3,t} < p_{2,t}$ (dash-dotted). Here $y_1, y_2 \in (-5, 5)$.

We have also tried another option to cut off the singularity:

$$|\vec{p}_{1,t} + \vec{p}_{2,t}| > \Delta_V . \quad (17)$$

This type of the cut will be called vector one for brevity. In Fig.16 we show corresponding photon-jet azimuthal angle correlation function with different values of the cut $\Delta_V = 0, 1, 2, 3$ GeV. The situation here is very similar to that for the scalar cut.

IV. CONCLUSIONS

We have performed for the first time the lacking in the literature calculation of the photon-jet correla-

tion observables in proton-proton (RHIC) and proton-

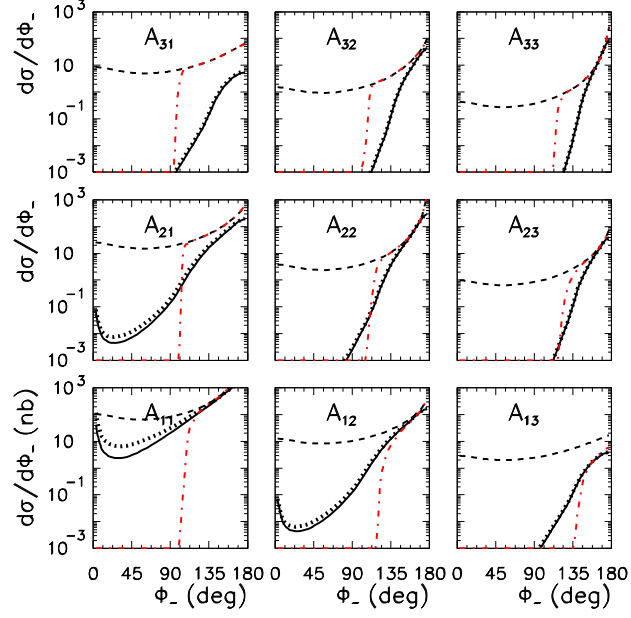


FIG. 11: Angular azimuthal correlations $d\sigma/d\phi_-$ at $\sqrt{s} = 1960$ GeV for Kwieciński on-shell ME (solid), Kwieciński off-shell ME (thick dotted), NLO collinear with no cuts on $p_{3,t}$ (dashed) and NLO collinear with cut on $p_{3,t} < p_{2,t}$ (dash-dotted). Here $y_1, y_2 \in (-5, 5)$.

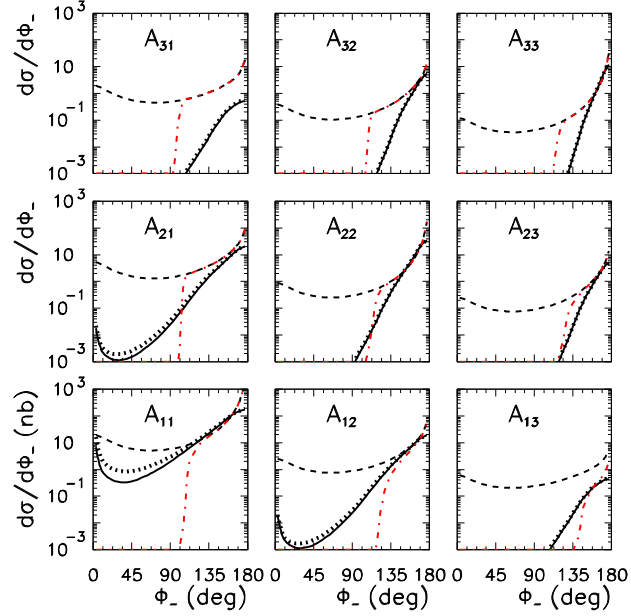


FIG. 12: Angular azimuthal correlations $d\sigma/d\phi_-$ at $\sqrt{s} = 1960$ GeV for Kwieciński on-shell ME (solid), Kwieciński off-shell ME (thick dotted), NLO collinear with no cuts on $p_{3,t}$ (dashed) and NLO collinear with cut on $p_{3,t} < p_{2,t}$ (dash-dotted). Here $|y_1|, |y_2| < 0.9$.

antiproton (Tevatron) collisions. Up to now such correlations have not been studied experimentally either. We

have concentrated on the region of small transverse momenta (semi-hard region) where the k_t -factorization ap-

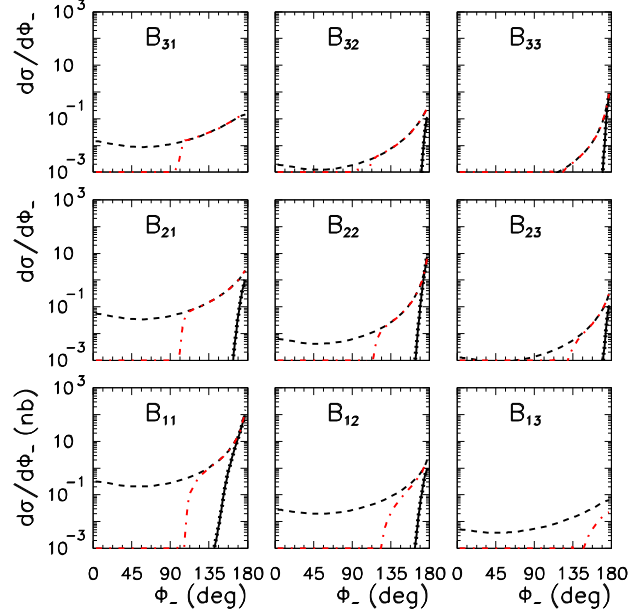
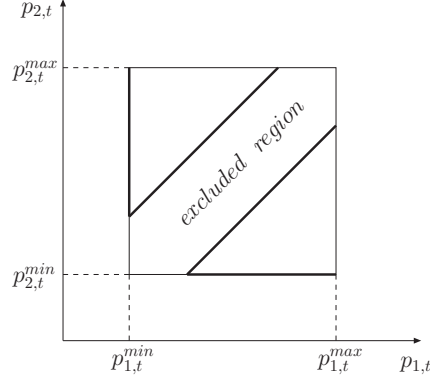


FIG. 13: Angular azimuthal correlations $d\sigma/d\phi_-$ at $\sqrt{s} = 1960$ GeV for Kwieciński on-shell ME (solid), Kwieciński off-shell ME (thick dotted) NLO collinear with no cuts on $p_{3,t}$ (dashed) and, NLO collinear with cut on $p_{3,t} < p_{2,t}$ (dash-dotted). Here $y_1, y_2 \in (-5, 5)$.



(a)

FIG. 14: Diagram showing excluded region in $(p_{1,t}, p_{2,t})$ plane.

proach seems to be the most efficient and theoretically justified tool. We have calculated correlation observables for different unintegrated parton distributions from the literature. Our previous analysis of inclusive spectra of direct photons suggests that the Kwieciński distributions give the best description at low and intermediate energies. We have discussed the role of the evolution scale of the Kwieciński UPDFs on the azimuthal correlations. In general, the bigger the scale the bigger decorrelation in

azimuth is observed. When the scale $\mu^2 \sim p_t^2$ (photon) $\sim p_t^2$ (associated jet) (for the kinematics chosen $\mu^2 \sim 100$ GeV²) is assumed, much bigger decorrelations can be observed than from the standard Gaussian smearing prescription often used in phenomenological studies.

The correlation function depends strongly on whether it is the correlation of the photon and any jet or the correlation of the photon and the leading-jet which is considered. In the last case there are regions in azimuth and/or

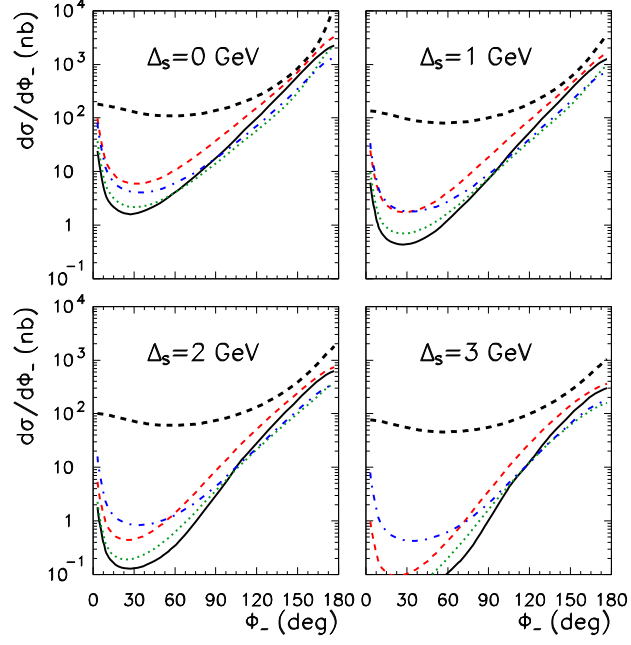


FIG. 15: Angular azimuthal correlations $d\sigma/d\phi_-$ at $\sqrt{s} = 1960$ GeV for different (scalar) cuts $\Delta_S = 0, 1, 2, 3$ GeV for NLO collinear (dashed), Kwieciński (solid), BFKL (dashed), KL (dotted) and KMR (dash-dotted). Here $p_{1,t}, p_{2,t} \in (5, 20)$ GeV and $y_1, y_2 \in (-5, 5)$.

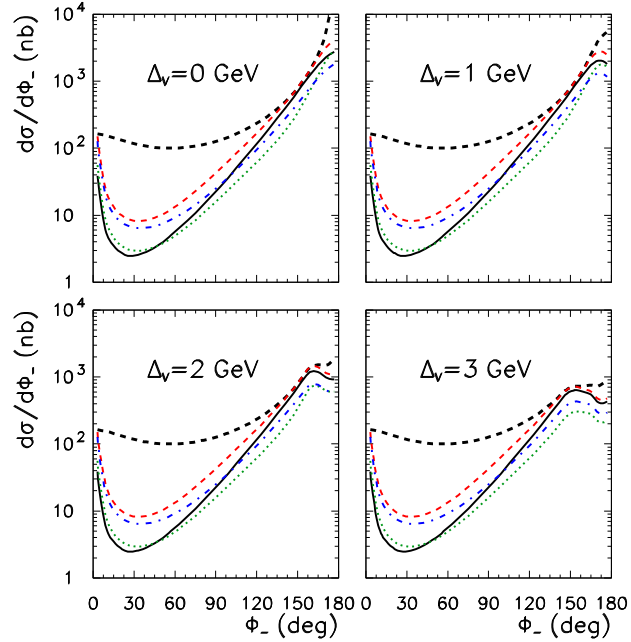


FIG. 16: Angular azimuthal correlations $d\sigma/d\phi_-$ at $\sqrt{s} = 1960$ GeV for different (vector) cuts $\Delta_V = 0, 1, 2, 3$ GeV for NLO collinear (dashed), Kwieciński (solid), BFKL (dashed), KL (dotted) and KMR (dash-dotted). Here $p_{1,t}, p_{2,t} \in (5, 20)$ GeV and $y_1, y_2 \in (-5, 5)$.

in the two-dimensional $(p_{1,t}, p_{2,t})$ space which cannot be populated in the standard next-to-leading order approach. In the latter case the k_t -factorization seems to be a useful and efficient tool.

We believe that the photon-jet correlations can be measured at Tevatron. At RHIC one can measure jet-hadron correlations for rather not too high transverse momenta of the trigger photon and of the associated hadron. This is precisely the semihard region discussed here. In this case the theoretical calculations would require inclusion of the fragmentation process. This can be done easily assuming independent parton fragmentation method using fragmentation functions extracted from e^+e^- collisions. This will be a subject of the following analysis.

Acknowledgments We are indebted to Jan Rak from the PHENIX collaboration for the discussion of recent results for photon-hadron correlations at RHIC. This work was partially supported by the grant of the Polish Ministry of Scientific Research and Information Technology number 1 P03B 028 28.

V. APPENDIX

A. Matrix elements for $2 \rightarrow 2$ processes with initial off-shell partons

In this paper we include four $2 \rightarrow 2$ processes such as $q\bar{q} \rightarrow \gamma g, \bar{q}q \rightarrow \gamma g, gq \rightarrow \gamma q, qg \rightarrow \gamma q$ important at midrapidity and relatively small transverse momenta. The corresponding matrix elements for the on-shell initial partons read

$$\begin{aligned} |\overline{\mathcal{M}}_{q\bar{q} \rightarrow \gamma g}|^2 &= \pi\alpha_{em}\sqrt{\alpha_{1,s}\alpha_{2,s}}(16\pi) \left(\frac{8}{9}\right) \left(\frac{\hat{u}}{\hat{t}} + \frac{\hat{t}}{\hat{u}}\right), \\ |\overline{\mathcal{M}}_{\bar{q}q \rightarrow \gamma g}|^2 &= \pi\alpha_{em}\sqrt{\alpha_{1,s}\alpha_{2,s}}(16\pi) \left(\frac{8}{9}\right) \left(\frac{\hat{t}}{\hat{u}} + \frac{\hat{u}}{\hat{t}}\right), \\ |\overline{\mathcal{M}}_{gq \rightarrow \gamma q}|^2 &= \pi\alpha_{em}\sqrt{\alpha_{1,s}\alpha_{2,s}}(16\pi) \left(-\frac{1}{3}\right) \left(\frac{\hat{u}}{\hat{s}} + \frac{\hat{s}}{\hat{u}}\right), \\ |\overline{\mathcal{M}}_{qg \rightarrow \gamma q}|^2 &= \pi\alpha_{em}\sqrt{\alpha_{1,s}\alpha_{2,s}}(16\pi) \left(-\frac{1}{3}\right) \left(\frac{\hat{t}}{\hat{s}} + \frac{\hat{s}}{\hat{t}}\right). \end{aligned}$$

The matrix elements for the off-shell initial partons were derived in Ref.[7]. To a good approximation the matrix elements for the off-shell initial partons can be also obtained by using the on-shell formulae (18) but with $\hat{s}, \hat{t}, \hat{u}$ calculated including off-shell initial kinematics. In this case $\hat{s} + \hat{t} + \hat{u} = k_1^2 + k_2^2$, where $k_1^2, k_2^2 < 0$ denote virtualities of initial partons. Our prescription can be treated as a smooth analytic continuation of the on-shell formula off mass shell. With our choice of initial parton four-momenta $k_1^2 = -k_{1,t}^2$ and $k_2^2 = -k_{2,t}^2$.

Explicit formulae for exact off-shell matrix elements were calculated and can be found in Ref.[7]. In this paper we compare results obtained with both (approximate and exact) ways.

B. Matrix elements for $2 \rightarrow 3$ processes

In order to obtain parton-parton $\rightarrow \gamma$ -jet matrix elements for the next-to-leading order one can use the following expression

$$\begin{aligned} \frac{1}{4} \sum_{spins} \frac{1}{N_C} \sum_{col} |M|^2 &= C_F 4\pi\alpha e_q^2 g_{1,s}^2 g_{2,s}^2 \\ &\times \left[2(C_F - \frac{1}{2}N_C)a_4 + N_C \frac{a_2 a_7 + a_3 a_6}{a_9} \right] \\ &\times \left[\frac{a_1^2 + a_5^2}{a_2 a_3 a_6 a_7} + \frac{a_2^2 + a_6^2}{a_1 a_3 a_5 a_7} + \frac{a_1^3 + a_7^2}{a_1 a_2 a_5 a_6} \right] \end{aligned}$$

for the $\gamma(p_1) + q(p_2) \rightarrow g(k_1) + g(k_3) + q(k_2)$ process obtained in [5]. Here $C_F = 4/3$, $N_C = 3$, where

$$\begin{aligned} g_{1,s}^2 &= 4\pi\alpha_s(p_{1,t}^2) \\ g_{2,s}^2 &= 4\pi\alpha_s(p_{2,t}^2) \end{aligned}$$

and

$$\begin{aligned} a_1 &= p_2 \cdot p_1, \quad a_5 = k_2 \cdot p_1, \quad a_8 = k_3 \cdot p_1, \quad a_{10} = k_1 \cdot p_1, \\ a_2 &= p_2 \cdot k_1, \quad a_6 = k_2 \cdot k_1, \quad a_9 = k_3 \cdot k_1, \\ a_3 &= p_2 \cdot k_3, \quad a_7 = k_2 \cdot k_3, \\ a_4 &= p_2 \cdot k_2, \end{aligned}$$

are redundant invariants. The longitudinal momentum fractions are calculated as:

$$\begin{aligned} x_1 &= (p_{1,t}e^{-y_1} + p_{2,t}e^{-y_2} + p_{3,t}e^{-y_3})/\sqrt{s} \\ x_2 &= (p_{1,t}e^{y_1} + p_{2,t}e^{y_2} + p_{3,t}e^{y_3})/\sqrt{s} \end{aligned}$$

As an example the expression for matrix elements for the second diagram

$$g(p_1) + g(p_2) \rightarrow \gamma(k_1) + q(k_3) + \bar{q}(k_2)$$

in Fig.2(b) we get from

$$\underbrace{\gamma(p_1)} + \underbrace{q(p_2)} \rightarrow \underbrace{g(k_1)} + \underbrace{g(k_3)} + \underbrace{q(k_2)}$$

diagram (see Fig.17) if we make the following replacement

$$\begin{aligned} p_1 &\rightarrow k_1, \\ k_1 &\rightarrow p_1, \\ p_2 &\rightarrow k_3, \\ k_3 &\rightarrow p_2, \end{aligned}$$

thus obtaining:

$$\begin{aligned} a_1 &\rightarrow a_9, \quad a_5 \rightarrow a_6, \quad a_8 \rightarrow a_2, \quad a_{10} \rightarrow a_{10}, \\ a_2 &\rightarrow a_8, \quad a_6 \rightarrow a_5, \quad a_9 \rightarrow a_1, \\ a_3 &\rightarrow a_3, \quad a_7 \rightarrow a_4, \\ a_4 &\rightarrow a_7, \end{aligned}$$

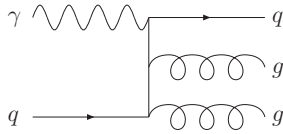


FIG. 17: Diagram of the $\gamma q \rightarrow ggq$ process.

-
- [1] S.S. Adler et al. (PHENIX collaboration), Phys. Rev. Lett. **97** (2006) 052301;
 S.S. Adler et al. (PHENIX collaboration), Phys. Rev. **C73** (2006) 054903;
 S.S. Adler et al. (PHENIX collaboration), Phys. Rev. Lett. **96** (2006) 222301;
 M. Oldenburg et al. (STAR collaboration), Nucl. Phys. **A774** (2006) 507.
- [2] S.S. Adler et al. (PHENIX collaborations), Phys. Rev. **D74** (2006) 072002.
- [3] DongJo Kim, a talk at the international workshop on “High- p_t processes at LHC”, Jyväskylä, Finland, March 23-28, 2007.
- [4] F.A. Berends, R. Kleiss, P.De Causmaecker, R. Gastmans and T.T. Wu, Phys. Lett. **B 103** 124 (1981).
- [5] P. Aurenche, A. Baier, A. Douiri, M. Fontannaz and D. Schiff, Nucl. Phys. **B286** 553 (1987).
- [6] T. Pietrycki and A. Szczurek, Phys. Rev. **D75** 014023 (2007).
- [7] A.V. Lipatov and N.P. Zotov, Phys. Rev. **D72** 054002 (2005);
 A.V. Lipatov and N.P. Zotov, hep-ph/0507243.
- [8] C. B. Mariotto, M. B. Gay Ducati and M. V. T. Machado, Phys. Rev. **D 66** 114013 (2002) [arXiv:hep-ph/0208155].
- [9] M. Luszczak and A. Szczurek, Phys. Lett. **B 594** 291 (2004).
- [10] S.P. Baranov and M. Smizanska, Phys. Rev. **D62** 014012 (2000).
- [11] M. Luszczak and A. Szczurek, arXiv:hep-ph/0512120, Phys. Rev. **D73** 054028 (2006).
- [12] P. Hagler, R. Kirschner, A. Schafer, L. Szymanowski and O. V. Teryaev, Phys. Rev. **D 63** 077501 (2001) [arXiv:hep-ph/0008316].
- [13] P. Hagler, R. Kirschner, A. Schafer, L. Szymanowski and O. V. Teryaev, Phys. Rev. Lett. **86** 1446 (2001) [arXiv:hep-ph/0004263].
- [14] J. Kwieciński and A. Szczurek, Nucl. Phys. **B680** 164 (2004).
- [15] A. V. Lipatov and N. P. Zotov, Eur. Phys. J. **C 44** 559 (2005) [arXiv:hep-ph/0501172];
 A. V. Lipatov and N. P. Zotov, arXiv:hep-ph/0510043.
- [16] M. Luszczak and A. Szczurek, hep-ph/0504119, Eur. Phys. J. **C46** 123 (2006).
- [17] J. Kwieciński, Acta Phys. Polon. **B33** 1809 (2002);
 A. Gawron and J. Kwieciński, Acta Phys. Polon. **B34** 133 (2003);
 A. Gawron, J. Kwieciński and W. Broniowski, Phys. Rev. **D68** 054001 (2003).
- [18] M.A. Kimber, A.D. Martin and M.G. Ryskin, Phys. Rev. **D63** 114027 (2001).
- [19] J.F. Owens, Rev. Mod. Phys. **59** 465 (1987).
- [20] U. d’Alesio and F. Murgia, Phys. Rev. **D70** 074009 (2004).
- [21] M. Glück, E. Reya and A. Vogt, Eur. Phys. J. **C5** 461 (1998).